Supplement of Geosci. Model Dev., 18, 3623–3634, 2025
https://doi.org/10.5194/gmd-18-3623-2025-supplement

Geoscientific Model Development
Open Access

Supplement of

A novel method for quantifying the contribution of regional transport to $PM_{2.5}$ in Beijing (2013–2020): combining machine learning with concentration-weighted trajectory analysis

Kang Hu et al.

Correspondence to: Hong Liao (hongliao@nuist.edu.cn)

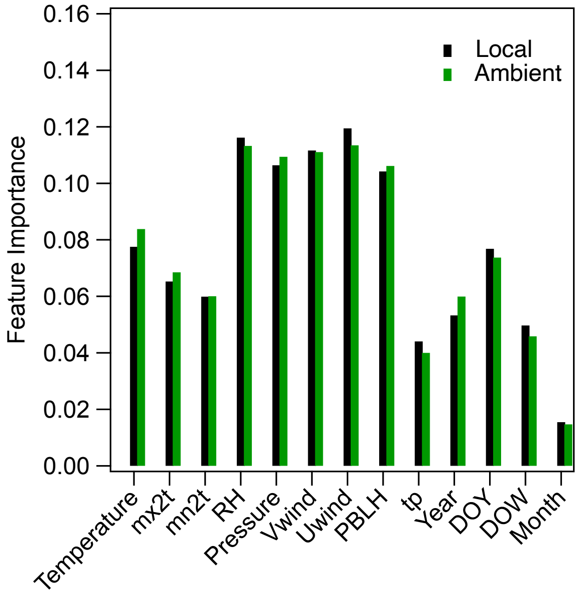

Fig. S1. Feature importance of the XGBoost models in estimating local (black) and ambient (green) $PM_{2.5}$ using the training data. The considered features include temperature, 2-m maximum (mx2t), 2-m minimum temperature (mn2t), relative humidity (RH), surface pressure, V-wind, U-wind, planetary boundary layer height (PBLH), total precipitation (tp), year, day of year, day of week, and month.

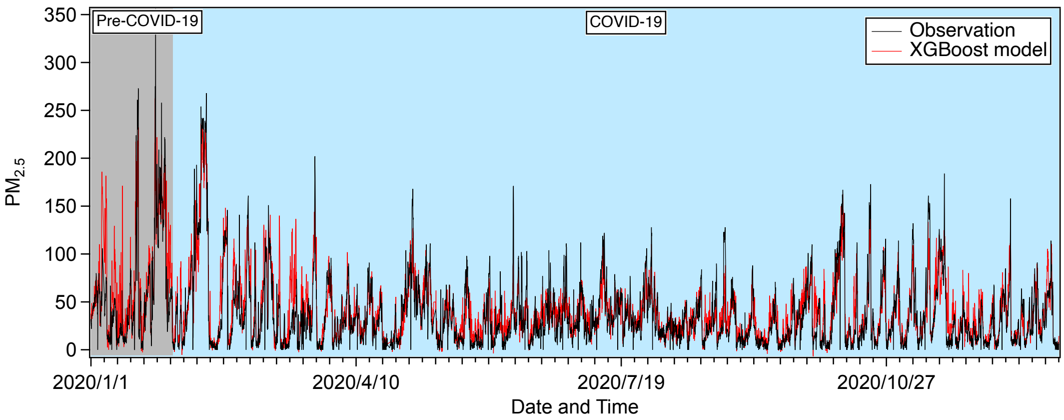

Fig. S2. Temporal evolution of $PM_{2.5}$ observations (black lines) and XGBoost model predictions (red lines) using testing data. The grey and blue shades represent the periods pre-COVID-19 and during COVID-19, respectively.

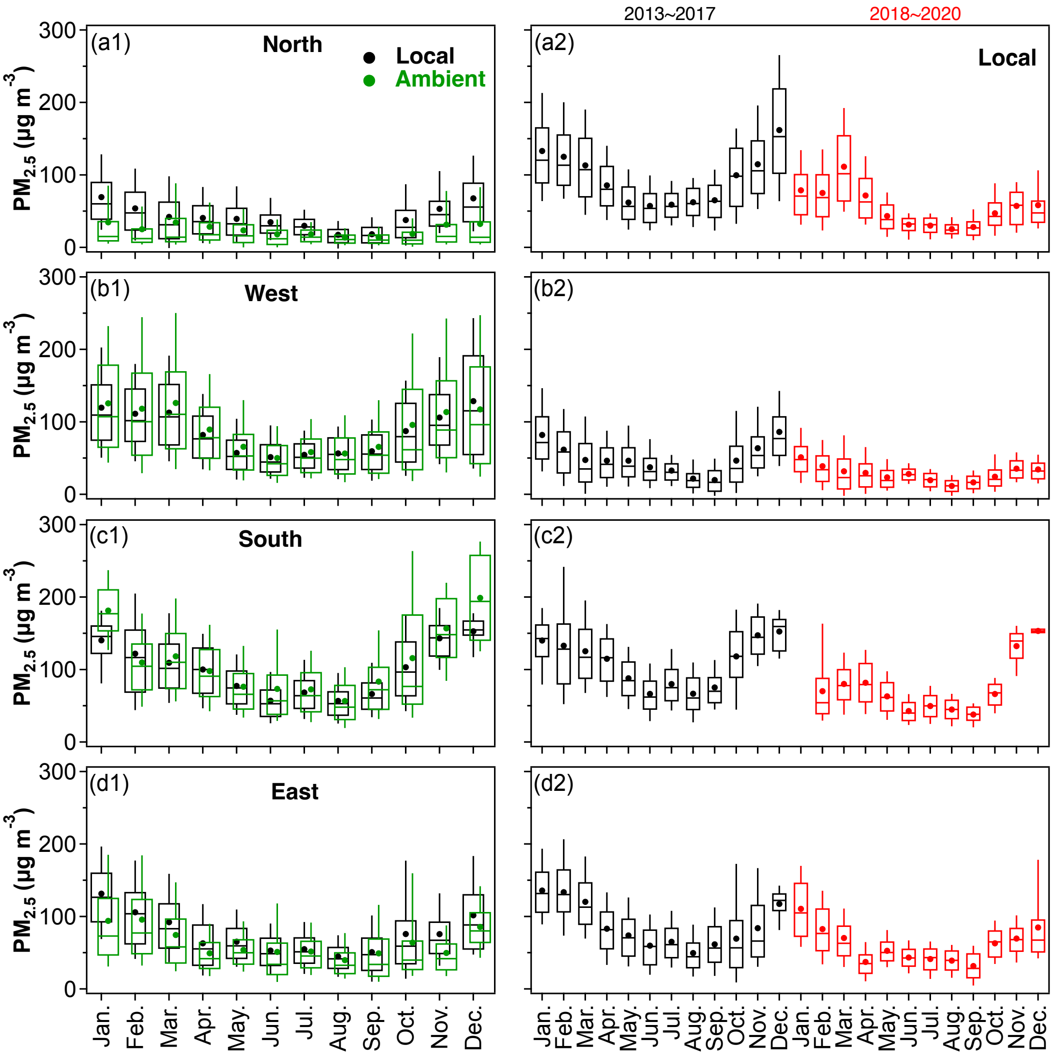

Fig. S3. Monthly variations of local (black) and ambient (green) $PM_{2.5}$ from the (a1) North, (b1) West, (c1) South, and (d1) East regions during 2013-2020. Right panels show monthly variations of local $PM_{2.5}$ before (black) and after (red) 2017 for the corresponding source regions in the left panels. The upper and lower boundaries represent the 75th and 25th percentiles, respectively, while the solid origin represents the average value.

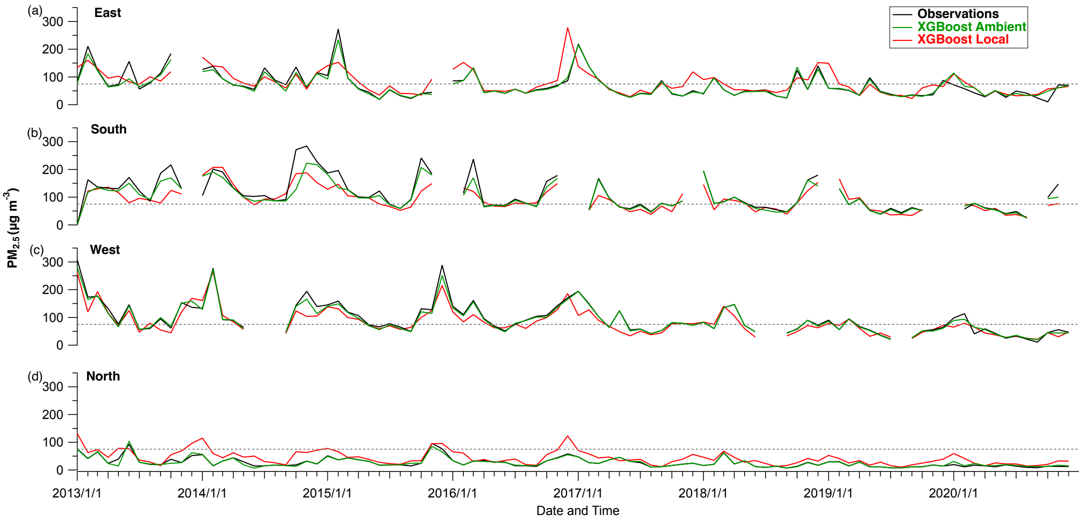

Fig. S4. Temporal variations of monthly $PM_{2.5}$ from the (a) East, (b) South, (c) West, and (d) North regions. Black, green, and red lines represent observations, XGBoost model results for ambient $PM_{2.5}$, and local $PM_{2.5}$, respectively. The horizontal dash line represents a $PM_{2.5}$ concentration of 75 μg m^{-3}.

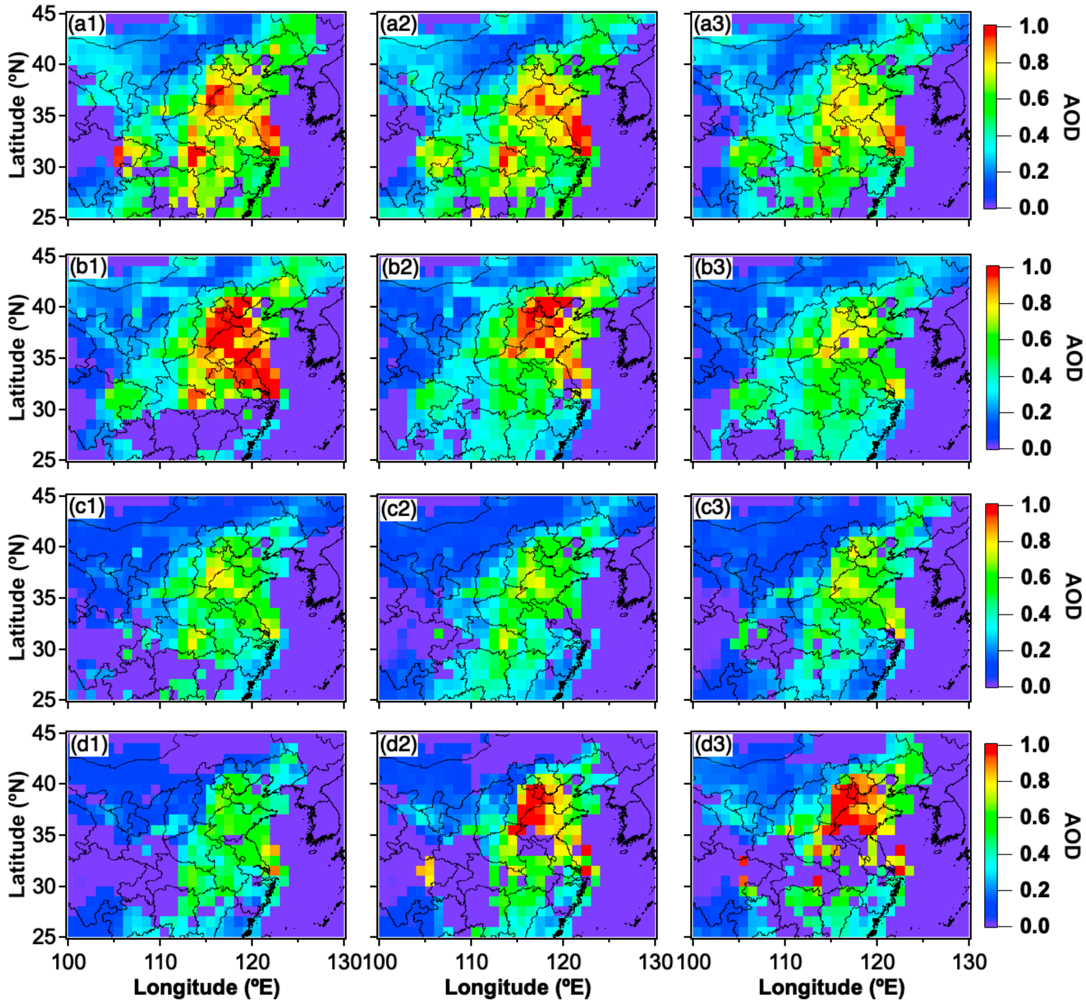

Fig. S5. Spatial climatology of monthly mean aerosol optical depth (AOD) at 550 nm based on daily Collection 6 (C006) combined Dark Target and Deep Blue MODIS Aqua retrievals for (a1) March, (a2) April, (a3) May, (b1) June, (b2) July, (b3) August, (c1) September, (c2) October, (c3) November, (d1) December, (d2) January, and (d3) February.

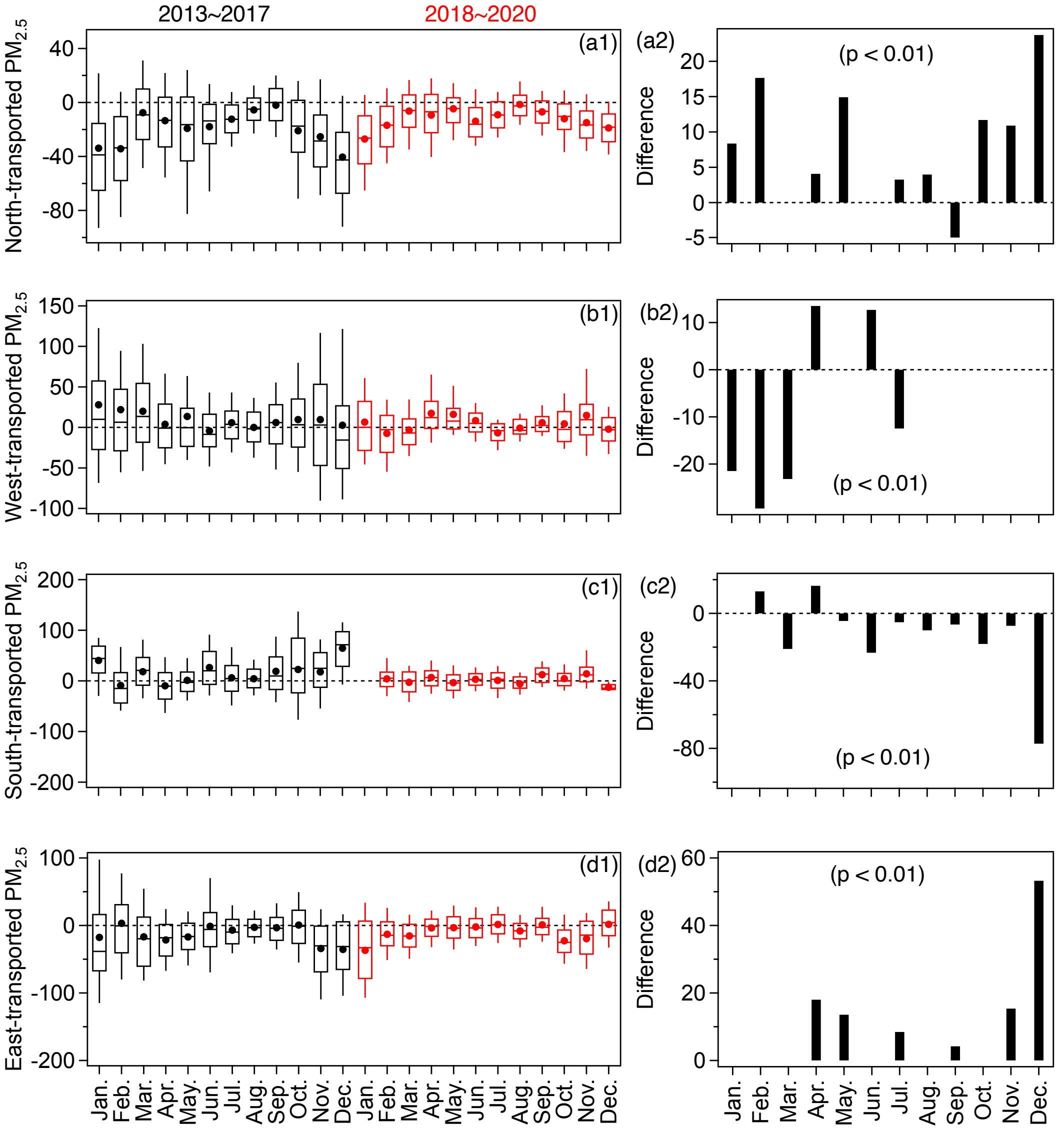

Fig. S6. Monthly variations of $PM_{2.5}$ transmitted from the (a1) North, (b1) West, (c1) South, and (d1) East regions during 2013-2017 (black) and 2018-2020 (red). The upper and lower boundaries represent the 75th and 25th percentiles, respectively, while the solid origin represents the average value. The right panels display the absolute change in monthly average differences between the periods 2013-2017 and 2018-2020. Only results passing the *t*-test ($p < 0.01$) are shown.

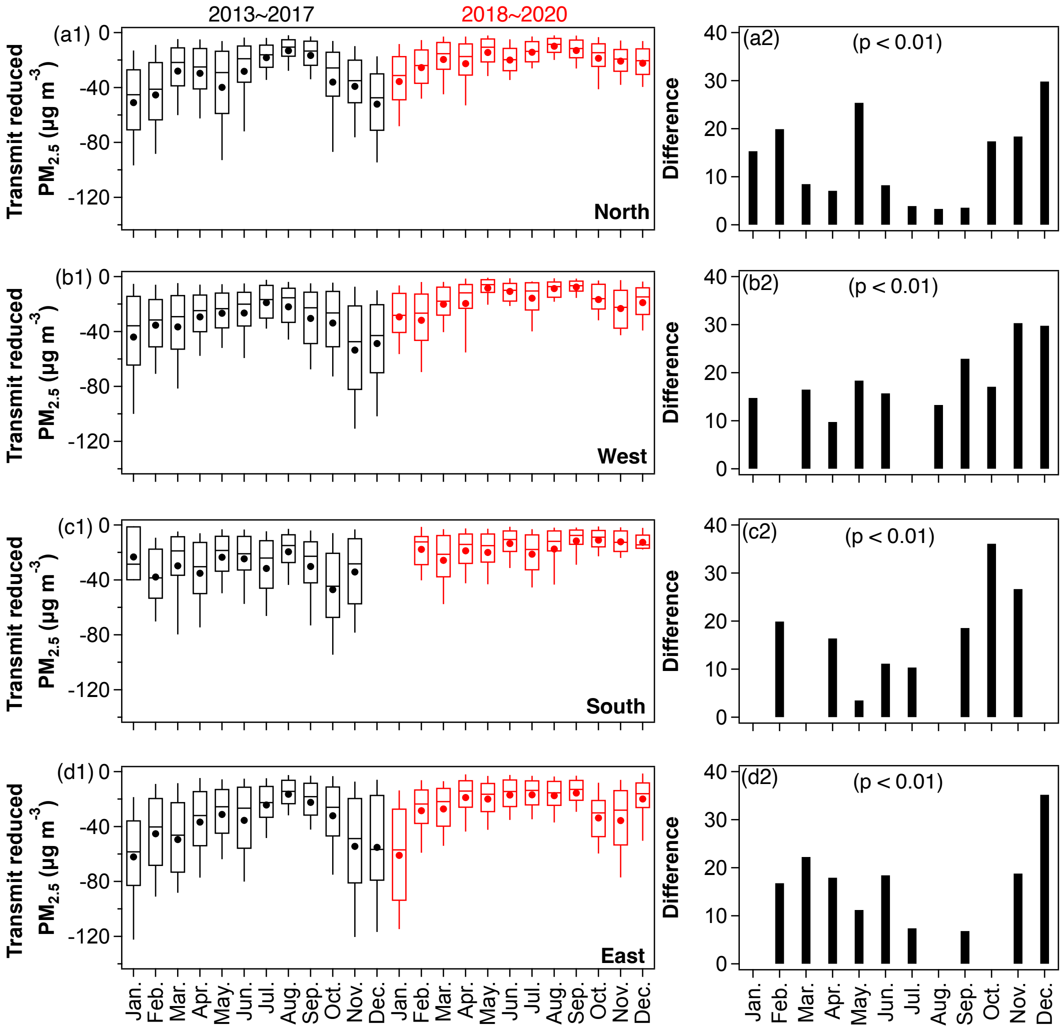

Fig. S7. Legend identical to that of Fig. S3, but for $PM_{2.5}$ reductions caused by regional transport.

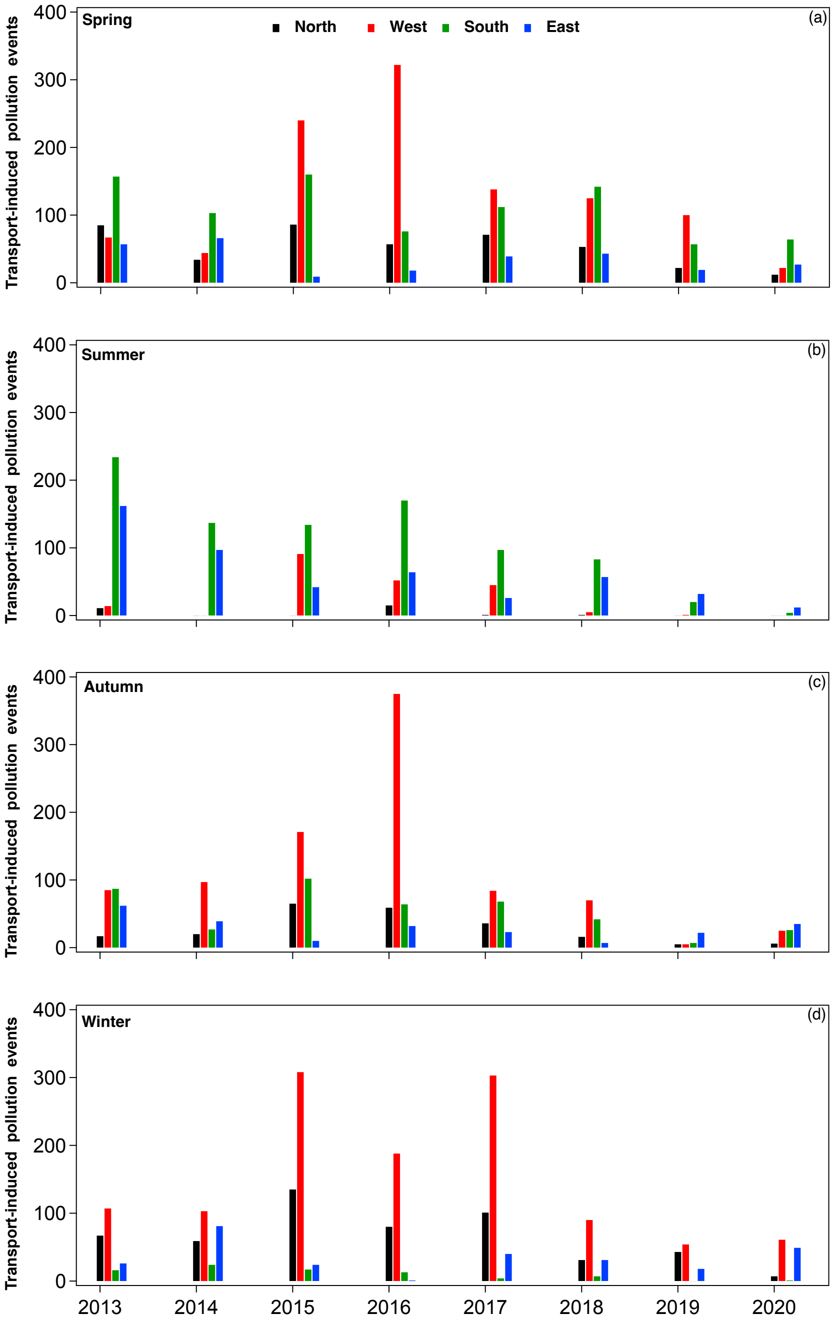

Fig. S8. Number of regional transport pollution events in each direction from 2013 to 2020 during (a) spring, (b) summer, (c) autumn, and (d) winter.

Table S1. Number of pollution events caused by local emissions and regional transport in Beijing during spring.

	2013~2017	2018~2020	2013~2020
Total	3944	1407	5351
Regional transport	1941	686	2627
Local	2003	721	2724
Regional transport / Local	0.97	0.95	0.96

Table S2. Identical legends to Table S1 but for summer.

	2013~2017	2018~2020	2013~2020
Total	3223	381	3604
Regional transport	1392	215	1607
Local	1831	166	1997
Regional transport / Local	0.76	1.3	0.8

Table S3. Identical legends to Table S1 but for autumn.

	2013~2017	2018~2020	2013~2020
Total	3906	885	4791
Regional transport	1523	266	1789
Local	2383	619	3002
Regional transport / Local	0.64	0.43	0.6

Table S4. Identical legends to Table S1 but for winter.

	2013~2017	2018~2020	2013~2020
Total	4694	1395	6089
Regional transport	1697	392	2089
Local	2997	1003	4000
Regional transport / Local	0.57	0.39	0.52